HHS Public Access

Author manuscript

J Alzheimers Dis. Author manuscript; available in PMC 2016 April 12.

Published in final edited form as:

J Alzheimers Dis. 2015 ; 47(4): 1021–1033. doi:10.3233/JAD-150242.

Bivalent compound 17MN exerts neuroprotection through interaction at multiple sites in a cellular model of Alzheimer's disease

Kai Liu[a,§], **Jeremy E. Chojnacki**[a,§], **Emily E. Wade**[a], **John M. Saathoff**[a], **Edward J. Lesnefsky**[b,c], **Qun Chen**[b], and **Shijun Zhang**[a,*]

[a]Department of Medicinal Chemistry, Virginia Commonwealth University, Richmond, VA, 23298

[b]Department of Medicine, Pauley Heart Center, Division of Cardiology, Virginia Commonwealth University, Richmond, VA, 23298

[c]Biochemistry, Virginia Commonwealth University, Richmond, VA, 23298

Abstract

Multiple pathogenic factors have been suggested in playing a role in the development of Alzheimer's disease (AD). The multifactorial nature of AD also suggests the potential use of compounds with polypharmacology as effective disease-modifying agents. Recently, we have developed a bivalent strategy to include cell membrane anchorage into the molecular design. Our results demonstrated that the bivalent compounds exhibited multifunctional properties and potent neuroprotection in a cellular AD model. Herein, we report the mechanistic exploration of one of the representative bivalent compounds, 17MN, in MC65 cells. Our results established that MC65 cells die through a necroptotic mechanism upon the removal of tetracycline (TC). Furthermore, we have shown that mitochondrial membrane potential (MMP) and cytosolic Ca^{2+} levels are increased upon removal of TC. Our bivalent compound 17MN can reverse such changes and protect MC65 cells from TC removal induced cytotoxicity. The results also suggest that 17MN may function between the Aβ species and RIPK1 in producing its neuroprotection. Colocalization studies employing a fluorescent analog of 17MN and confocal microscopy demonstrated the interactions of 17MN with both mitochondria and endoplasmic reticulum (ER), thus suggesting that 17MN exerts its neuroprotection via a multiple-site mechanism in MC65 cells. Collectively, these results strongly support our original design rationale of bivalent compounds and encourage further optimization of this bivalent strategy to develop more potent analogs as novel disease-modifying agents for AD.

Keywords

Alzheimer's disease; bivalent compound; neuroprotection; mitochondria; calcium; multifunctional

[*]Correspondence address: Shijun Zhang, Ph.D., Department of Medicinal Chemistry, School of Pharmacy, Virginia Commonwealth University, Richmond, VA 23298, Tel: 8046288266, Fax: 8048287625, szhang2@vcu.edu.

[§]These authors contributed equally to the manuscript.

INTRODUCTION

It is estimated that 5.2 million Americans of all ages and up to 30 million individuals worldwide are affected by Alzheimer's disease (AD), a devastating neurodegenerative disorder and the most common cause of dementia.[1] Although significant advances have been made in understanding the mechanisms leading to AD, the complexity of this disease still remains since multiple pathogenic factors have been implicated in its development. This includes amyloid-β (Aβ) aggregates, [2] soluble Aβ oligomers (AβOs), [3–5] dyshomeostasis of biometals, oxidative stress, neuroinflammation, and mitochondrial dysfunction, among others.[6–8] As a result, drug development efforts to provide effective disease-modifying agents for AD still remain a challenging and unmet task since the traditional "one molecule, one target" drug discovery approach may not fit the multifactorial nature of AD. To address this challenge, the multifunctional strategy of small molecule design has recently attracted extensive attention in surmounting the paucity of effective disease-modifying agents in the pipeline of AD therapeutics.[9–11] However, rational design of small molecules with therapeutic polypharmacology has always been a challenging task as it involves the selection of suitable screening assays and the validation of engagement of multiple targets by the designed molecules.

Recently, we developed a novel bivalent ligand strategy by linking a multifunctional "war head" with a cell membrane/lipid raft anchor moiety and incorporated this approach into our molecular design.[12, 13] Our results demonstrated that the bivalent compounds exhibit significantly improved neuroprotection compared to the "war head" and the CM/LR anchor alone, or the combination of these two. Furthermore, we have demonstrated that the spacer length between the "war head" and the anchorage moiety is critical for neuroprotection. However, the exact mechanism of action remains elusive. In the characterization of these compounds, we employed MC65 cells as our primary phenotypic screening assay to confirm neuroprotective activity. MC65 cells are a human neuroblastoma cell line that conditionally expresses C99, the C-terminus fragment of amyloid-β protein precursor (APP), using tetracycline (TC) as a transgene suppressor.[14] Although limited mechanistic studies have been conducted to show that intracellular Aβ aggregates, including small AβOs, along with oxidative stress gradually lead to cell death, [14–16] the mechanism of cell death still remains unknown. Therefore, further understanding of the pathway of cell death of MC65 cells, along with the detailed charaterization of the mechanisms of action of the designed bivalent compounds, would greatly facilitate the application of this cellular AD model to AD drug discovery and the development of more potent bivalent compunds. Herein, we report the characterization of the mechanism of MC65 cell death upon withdrawal of TC, and the related involvement of mitochondria, endoplasmic reticulum, and calcium mobilization. We also investigated how our bivalent compounds affect these processes and the preliminary mechanisms for their neuroprotective activity.

MATERIAL AND METHODS

Cell Lines and Reagents

MC65 cells (kindly provided by Dr. George M. Martin at the University of Washington, Seattle) were cultured in Dulbecco's Modified Eagle's Medium (DMEM) (Life

Technologies, Inc., Grand Island, NY) supplemented with 10% of heat-inactivated fetal bovine serum (FBS) (Hyclone, Logan, UT), 1% Penicillin/Streptomycin (P/S) (Invitrogen), 1 μg/mL Tetracycline (TC) (Sigma Aldrich, St. Louis, MO), and 0.2 mg/mL G418 (Invitrogen). SH-SY5Y cells (ATCC) were cultured in DMEM supplemented with 10% FBS and 1% P/S. All cells were maintained at 37 °C in a fully humidified atmosphere containing 5% CO_2.

MC65 Apoptosis assay

MC65 cells were collected and washed twice with PBS, resuspended in Opti-MEM, seeded in 6-well plates (1.6×10^6 cells/well), and incubated with compounds at 37 °C under −TC conditions for 48 h. Cells were harvested and washed twice with cold PBS, and then suspended in 1x binding buffer (10 mM HEPES [N-2-hydroxyethylpiperazine-N′-2-ethanesulfonic acid] (pH 7.4), 140 mM NaOH, 2.5 mM $CaCl_2$). Annexin V-fluorescein isothiocyanate (FITC) (BD PharMingen, San Diego, CA) and 5 μg/mL propidium iodide (PI) were then added, and the cells were incubated in dark for 15 min at room temperature per the manufacturer's instructions. Samples were analyzed by flow cytometry using a Millipore Guava easyCyte flow cytometer.

Caspase 3 Western blot

MC65 cells (4×10^5 cells/mL) were treated under indicated conditions for 48 h, and then collected in cold PBS, lysed by sonication in a Tricine buffer solution, and boiled for 5 min. Protein samples were collected from the supernatant after centrifugation at 12,800×*g* for 5 min, and the concentrations were quantified using the Bradford method. Equal amounts of protein (20.0 μg) were separated by SDS-PAGE on a gel (Bio-Rad) and transferred onto a PVDF membrane (Bio-Rad). The blots were blocked with 5% milk in a TBS-0.1% Tween 20 (TBS-T) solution at room temperature for 1 h and then probed with the caspase 3 antibody (Cell Signaling Technology, Danvers, MA) overnight at 4 °C. The blots were washed twice in TBS-T for 15 min, and then incubated with a 1:1000 dilution of horseradish peroxidase-conjugated secondary antibody in a 5% milk/TBS-T solution at room temperature for 1 h. After washing twice in TBS-T for 15 min, the proteins were visualized by a Western Blot Chemiluminescence Reagent (Thermo Fischer Scientific, Waltham, MA). The blots were also probed with antibodies against α-tubulin to ensure equal loading of proteins.

MC65 Neuroprotection assay

MC65 cells were washed twice with PBS, resuspended in Opti-MEM, and seeded in 96-well plates (4×10^4 cells/well). Indicated compounds were then added, and cells were incubated at 37°C under −TC conditions for 72 h. Then, 10 μL of MTT solution (3-(4,5-Dimethylthiazol-2-yl)-2,5-diphenyltetrazolium bromide 5 mg/mL in PBS) were added and the cells were incubated for another 4 h. Cell medium was then removed, and the remaining formazan crystals produced by the cellular reduction of MTT were dissolved in 100 μL of DMSO. Absorbance at 570 nm was immediately recorded using a FlexStation 3 plate reader (Molecular Devices, CA). Values were expressed as a percentage relative to those obtained in the +TC controls.

Transmission Electron Microscopy

MC65 cells were collected and washed twice with PBS. The cells were suspended in Opti-MEM and incubated under −TC condition for 48 h. Cells were fixed with 2.5% Glutaraldehyde in 0.1 M Sodium Cacodylate Buffer. After being embedded, the sample was viewed with a Jeol JEM-1230 TEM (JEOL USA, MA).

U937 Necroptosis assay

U937 cells (2×10^4 cells) were pretreated with compound and pan caspase inhibitor zVAD for 1 h. TNF-α was then added and cells were incubated for 72 h. Afterward, 10 μL of MTT solution was added and cells were incubated for an additional 4 h. Cell medium was then removed, and the remaining formazan crystals produced by the cellular reduction of MTT were dissolved in 100 μL of DMSO. Absorbance at 570 nm was immediately recorded using a FlexStation 3 plate reader. Values were expressed as a percentage relative to those obtained in untreated controls.

$A\beta_{40}$ ELISA

MC65 cells were collected and washed twice with PBS, resuspended in Opti-MEM, seeded in 6-well plates (1.6×10^6 cells/well), and incubated with compounds at 37 °C under −TC conditions for 48 h. After centrifugation of the plates, 2 mL of medium were carefully collected for analysis of $A\beta_{40}$ in medium. Cell pellets were lysed by cell extraction buffer (Life Technologies) following the manufacturer's instructions and the total protein content was quantified by the Bradford method. Samples were analyzed using the $A\beta_{40}$ Human ELISA Kit (Life Technologies) following the manufacturer's instructions. The results were normalized by total protein expressed as a percentage relative to those obtained in the −TC control.

MC65 Mitochondrial membrane potential assay

MC65 cells were collected and washed twice with PBS, resuspended in Opti-MEM, seeded in 6-well plates (1.6×10^6 cells/well), and incubated with compounds at 37 °C under −TC conditions for 48 h. Cells were then collected, washed twice with PBS, and then incubated with 100 nM of tetramethylrhodamine methyl ester (TMRM) in PBS at room temperature for 30 min. Fluorescence was analyzed by flow cytometry.

SH-SY5Y Mitochondrial membrane potential assay

SH-SY5Y cells (4×10^5 cells) were plated in 12-well plates. After incubation for 24 h, growth medium was removed and cells were treated in DMEM with indicated compounds and MPP^+ (2.5 mM) for 24 h. TMRM was then added to a final concentration of 100 nM and the cells were further incubated for 30 min. The medium was then collected. Cells were detached by trypsinization, and the medium was then recombined with the cells and centrifuged. After removing the supernatant, the cell pellet was suspended in PBS and the mean fluorescent intensity was recorded by flow cytometry.

Brain mitochondrial isolation and functional determination

The Institutional Animal Care and Use Committees (IACUC) of the McGuire VA Medical Center and Virginia Commonwealth University approved this protocol. Brain cortex tissue was collected from C57BL/6 mice after the mouse was anesthetized with sodium pentobarbital (100 mg/kg i.p.) and the heart was removed. Harvested brain tissue was placed into 5 mL MSM buffer (210 mM Mannitol, 70 mM Sucrose, 5.0 mM MOPS, 1.0 mm EDTA, pH 7.4) at 4 °C, finely minced, and incubated with Subtilisin A (1 mg/g tissue) for 1 min. Another 5 mL MSM buffer including 0.2% BSA was added to incubated tissue that was then homogenized by one stroke using a Teflon pestle. The homogenate was centrifuged at 600×*g* for 10 min at 4 °C. The supernatant was then centrifuged at 5000×*g* for 10 min at 4 °C to spin down the mitochondria. The mitochondrial pellet was washed once with MSM buffer, then resuspended in 100–200 μL of MSM buffer. Total protein concentration was measured by the Lowry method using BSA as a standard. Oxygen consumption in mitochondria was measured by a Clark-type oxygen electrode at 30 °C using glutamate + malate (complex I substrates) and succinate + rotenone (complex II substrates) in the presence or absence of compound 17MN.[17]

MC65 Calcium level measurement

MC65 cells were washed twice with PBS, resuspended in Opti-MEM, and seeded in 6-well plates (1.6×10^6 cells/well). Indicated compounds were then added, and cells were incubated at 37 °C under −TC conditions for 48 h. Cells were then harvested, suspended in PBS, and incubated with Fluo-4AM (2 μM) in dark for 30 min. Cells were washed once and then resuspended in PBS. Samples were analyzed by flow cytometry. Values were expressed as a percentage relative to those obtained in −TC controls.

Biometal complex assay

Compound 17MN (50 μM) and $CaCl_2$ (60 μM) in water (100 μL) were incubated at room temperature for 10 min, then UV absorption was recorded from 300 nm to 600 nm using a Flexstation 3 plate reader.

MC65 Colocalization assay

MC65 cells were grown for 48 h on cover slides coated with polylysine. Cells were treated with the 17MN-NBD probe at 3 μM for 3.5 h. For mitochondrial visualization, Mitotracker Red (300 nM) was added and incubated for 30 min. Cells were washed twice with PBS and fixed with 4% formaldehyde for 30 min. After thrice washing with PBS, samples were mounted and solidified overnight, then analyzed by LSM710 confocal microscopy. For ER visualization, cells were rinsed once with HBSS buffer, and then ERtracker Red (1 μM) was incubated with cells in HBSS buffer for 30 min. Following the manufacturer's procedure, the staining solution was removed and cells were fixed with 4% formaldehyde for 5 min. Cells were then washed twice with HBSS buffer, mounted and solidified overnight, and then analyzed by LSM710 confocal microscopy.

Statistical analyses

The Student's t-test was used for all statistical analysis. Data are presented as mean ± SEM. The level of significance for all analysis testing was set at *P < 0.05.

RESULTS

MC65 cells die through necroptosis and bivalent compound 17MN engages targets downstream of Aβ aggregates and upstream of RIPK1

Studies have shown that, upon removal of TC, the aggregation of Aβ leads to extensive oxidative stress, and ultimately cell death in MC65 cells.[13, 15] But the exact mechanism of cell death remains unknown. Therefore, we decided to characterize the mechanisms of MC65 cell death. Firstly, we studied whether MC65 cells die through an apoptotic mechanism, as the literature has reported that Aβ can induce apoptosis in various cellular models.[18–20] Interestingly, as shown in Figure 1A, no apoptotic cell death was observed 48 h after the removal of TC, as reflected by no change in the percentage of cell populations on the lower and upper right quadrants, representing early and late apoptosis, respectively. This was also confirmed by western blot analysis of caspase 3 activation (Figure 1B). In order to compare these results with apoptotic cell death, we treated MC65 cells with $CoCl_2$, a known apoptosis inducer.[21] As shown in Supplementary Figure 1A, $CoCl_2$ induced significant early apoptosis after 48 h of treatment, as reflected by the change of cell population on the lower right quadrant (49.5% of $CoCl_2$ treated versus 7.5% of vehicle treated). Western blot analysis of caspase 3 activation also confirmed the induction of apoptosis as reflected by the appearance of the cleaved caspase 3 band (Supplementary Figure 1B). It has been reported that both extracellular and intracellular Aβ species can induce neuronal apoptosis via multiple mechanisms.[22–24] However, these current results suggest that MC65 cells adopt a different cellular environment that avoids apoptotic cell death upon accumulation of Aβ aggregates. Our recent studies have shown that, reactive oxygen species (ROS), especially mitochondrial ROS (mitoROS), are involved in the cell death of MC65 cells.[13, 25] It has also been shown that ROS could be effectors for necroptosis, a programmed cell necrosis.[26–28] Therefore, we set out to determine whether MC65 cells die through a necroptotic mechanism. To this end, we first tested whether necrostatin-1 (Nec-1), a specific receptor interacting protein kinase-1 (RIPK1) and necroptosis inhibitor, [29] could rescue MC65 cells from TC removal induced cell death. As shown in Figure 1C, Nec-1 dose-dependently protected MC65 cells, which indicates that necroptosis is involved in the cytotoxic effects of TC removal and consequent accumulation of Aβ aggregates. Morphological studies by transmission electron microscopy (TEM) also demonstrated a necroptotic mechanism of cell death (Figure 1D) as reflected by cell membrane rupture and the release of cellular contents. Further morphological examination also confirmed that Nec-1 can reverse the changes induced by the removal of TC back to a normal state (Supplementary Figure 2A). To rule out the possibility that the observed neuroprotective activities of Nec-1 could be due to its effects on the aggregation of Aβ upon TC removal, we first examined the aggregation of Aβ after 48 h of TC removal from MC65 cells pre-treated with Nec-1. As shown in Supplementary Figures 2B and 2C, surprisingly, Aβ aggregation was significantly suppressed by treatment of Nec-1 at concentrations of 10, 30, and 100 μM. However, Nec-1 at 3 μM did not show significant inhibition. When

compared with the neuroprotection results, Nec-1 at 3 μM significantly protected MC65 cells from TC removal induced cytotoxicity. This may suggest that the neuroprotective activity is still mainly through RIPK1; however, inhibition of RIPK1 by Nec-1 at higher concentrations may produce inhibitory effects on the aggregation of Aβ, as well. To further confirm this, we employed another experimental condition to test the engagement of RIPK1 by Nec-1 in exerting its neuroprotective activity. Our previous studies demonstrated that MC65 cells produce a significant amount of Aβ aggregates 27 h after TC removal.[12] Therefore, we treated MC65 cell with Nec-1 at 27 h after TC removal and measured the level of Aβ aggregates at 48 h after TC removal. As shown in Supplementary Figure 2D, Nec-1 treatment did not exhibit interference on Aβ aggregation under this experimental condition. Further cell viability assay results demonstrated that Nec-1 significantly protected MC65 cells upon treatment at 27 h after TC removal. Collectively, the results suggest that Nec-1 does not interfere with Aβ aggregation, and its neuroprotection is mainly through the engagement of RIPK1.

Since our bivalent compound 17MN (Figure 2A) efficiently protected MC65 cells from TC removal induced cytotoxicity, [13] we next wanted to investigate whether 17MN exerts its neuroprotective effects through targets upstream or downstream of RIPK1. To this end, we used the well-established U937 cell model of necroptosis induced by the presence of TNF-α and a pan caspase inhibitor, zVAD.[29, 30] As shown in Figure 2B, addition of TNF-α (50 ng/mL) and zVAD (10 μM) induced significant necroptotic cell death and Nec-1 protected U937 cells by 90% at 10 μM. However, 17MN did not show any protection up to 3 μM. This suggests that 17MN might interact with protein targets upstream of RIPK1 in MC65 cells since both 17MN and Nec-1 protected MC65 cells, but only Nec-1 protected U937 cells from TNF-α and zVAD induced necroptosis.

The accumulation of Aβ aggregates, including AβOs, in MC65 cells is a causative factor leading to cell death.[14] It has also been reported that the Aβ species produced in MC65 cells is mainly $A\beta_{40}$.[31] Therefore, to rule out the possibility that 17MN interferes with the production of Aβ, we examined the total level of $A\beta_{40}$ by ELISA assay. As shown in Figure 2C, 17MN (1 μM) slightly decreased the intracellular level of $A\beta_{40}$, but did not interfere with the level of extracellular $A\beta_{40}$. Overall, 17MN did not significantly inhibit the total production of $A\beta_{40}$, especially when comparing the reduction of intracellular $A\beta_{40}$ with the neuroprotective activity of 17MN at this concentration. Our previous studies demonstrated that 17MN exhibits inhibitory effects on the aggregation of small Aβ oligomers, but with a much weaker potency compared to its inhibition of MC65 cell death, thus suggesting that the inhibition of Aβ aggregation might only contribute partially towards its overall neuroprotective ability.[13] Taken together, the results from Figure 2, along with our previous results, suggest that bivalent compound 17MN mainly exerts its neuroprotective activities in MC65 cells by interacting with target proteins downstream of Aβ aggregates and upstream of RIPK1.

MC65 cells exhibit increased mitochondrial membrane potential and bivalent compound 17MN can reverse this increase

Our previous results showed that production of mitoROS is a contributing factor in the cell fate of MC65 cells, thus indicating a role of mitochondria in this cell model.[25] Aβ has also been shown to accumulate in mitochondria and affect their function.[32, 33] Furthermore, mitochondrial dysfunction has been linked with necroptosis, as well.[28, 34, 35] Therefore, we next examined the change of mitochondrial transmembrane potential (MMP, ΔΨm) upon the removal of TC. As shown in Figure 3A, interestingly, the ΔΨm increased after 48 h of TC removal. This is opposite to the reported results that exogenously applied Aβ decrease the ΔΨm.[36] Again, this highlights the fact that endogenously produced Aβ aggregates in MC65 cells interact with mitochondria differently under the current model conditions. Notably, 17MN suppressed the increase of ΔΨm at 0.1, 0.3, and 1 μM. This may indicate that our bivalent compounds interact with mitochondrial proteins and subsequently disrupt their potential interactions with AβOs. Since complex I of the electron transport chain is associated with the production of mitoROS, [37] we further employed another neuronal toxicity cell model, the SH-SY5Y cell line in the presence of MPP^+, to examine the effects of 17MN on ΔΨm. As shown in Figure 3B, the neurotoxin MPP^+ induced significant ΔΨm dissipation; however, 17MN did not reverse this change under these experimental settings. Since MPP^+ specifically targets complex I of the mitochondrial electron transport chain, these results might suggest that 17MN does not directly interact with the components of complex I, but instead, with other mitochondrial proteins that influence ΔΨm and the production of mitoROS. Next, we tested 17MN in isolated mouse brain mitochondria for its effects on oxyphosphorylation. As shown in Figures 3C and 3D, 17MN did not exhibit any significant effects on the oxidation of glutamate/malate and succinate, the substrates of complex I and complex II, respectively, in agreement with the results of SH-SY5Y assay. Studies have shown that mitochondrial membrane permeability transition (MPT) is associated with ΔΨm.[38, 39] Interestingly, TRO19622, a MPT modulator, is structurally similar to the cell membrane anchor moiety of 17MN.[40] Therefore, we examined whether TRO19622 can modulate the increased ΔΨm upon TC removal. As shown in Figure 4A, TRO19622 significantly suppressed the rise of ΔΨm at 10 μM, thus suggesting that MPT is associated with the ΔΨm in MC65 cells. However, when we examined whether TRO19622 can rescue MC65 cell death, the results revealed no protection (Figure 4B). This might indicate that the ΔΨm change in MC65 cells is a downstream event, rather than one of the causative factors, to the ultimate cytotoxicity. Also, this does not rule out the possibility that although TRO19622 can modulate ΔΨm, MPT is not associated with the cell death mechanism of MC65 cells upon removal of TC.

Cytosolic Ca^{2+} is increased upon TC removal in MC65 cells and 17MN can abolish this change

Ca^{2+} overload has been indicated in the induction of MPT, mitochondrial dysfunction, ROS production, and necroptosis.[41–43] Aβ aggregates have also been shown to play a role in the dyshomeostasis of Ca^{2+}.[44, 45] Therefore, we investigated changes in Ca^{2+} levels upon removal of TC in MC65 cells and whether 17MN had any effect on this change. As shown in Figure 5A, TC removal resulted in a significant rise of cytosolic Ca^{2+} as measured by Fluo-4AM, and interestingly, 17MN dose-dependently prevented this increase. Considering

17MN has shown the potential to form complexes with biometals Cu, Zn, and Fe, [13] we measured the complex formation between 17MN and Ca^{2+} to rule out the possibility that 17MN is simply chelating Ca^{2+} directly. As shown in Figure 5B, 17MN does not form a complex with Ca^{2+} as evidenced by no change in the absorption profile between 17MN alone and co-administration with Ca^{2+}. This suggests that 17MN reduces the increase of Ca^{2+} possibly through its interactions with target proteins. To further understand the origin of the Ca^{2+} rise, we employed various pharmacological inhibitors to study their effects in MC65 cells (Figure 6A). Depletion of extracellular Ca^{2+} by ethylene glycol tetraacetic acid (EGTA) did not prevent the intracellular rise, suggesting that the elevation is mediated through intracellular organelles. Therefore, we turned our attention to the endoplasmic reticulum (ER) and mitochondria, two main storage sites of Ca^{2+} and integral organelles in maintaining Ca^{2+} homeostasis. Notably, 2-aminoethoxydiphenyl borate (2-APB), an inositol 1,4,5-triphosphate receptor (IP_3R) channel inhibitor, completely reversed the TC removal induced Ca^{2+} increase, indicating that upon accumulation of Aβ aggregates, Ca^{2+} release from the ER is potentiated through store-operated channels and the IP_3R channel.[46, 47] Interestingly, the mitochondrial Ca^{2+} channel inhibitor, cyclosporine A, further increased the elevation of Ca^{2+} levels upon treatment of MC65 cells. It has been proposed that the transfer of Ca^{2+} between ER and mitochondria is mediated through the IP_3R linked Ca^{2+} channel and the voltage-dependent anion-selective channel protein 1 (VDAC1) on the mitochondria, a component of the mitochondrial permeability transition pore structure.[48–50] Considering this, our results might suggest that Aβ aggregates can trigger the release of Ca^{2+} from the ER, causing a shuffle of stored Ca^{2+} through mitochondria to balance intracellular levels. Upon inhibition of the mitochondrial permeability transition pore by cyclosporine A, Ca^{2+} cannot be taken back up into the mitochondria, leading to the previously observed elevation. To further understand whether the $\Delta\Psi m$ change is associated with the change of Ca^{2+} level, we investigated the effects of 2-APB on $\Delta\Psi m$. As shown in Figure 6B, treatment of MC65 cells with 2-APB did not affect the TC removal induced MMP rise. Next, we tested whether the antioxidant Trolox had any effect on Ca^{2+} since we have shown that Trolox can effectively protect MC65 cells.[12] Notably, as shown in Figure 6C, Trolox effectively suppressed the Ca^{2+} rise upon TC removal at 10 μM, a concentration at which significant neuroprotection was observed in MC65 cells. Taken together, these results may suggest that the change in Ca^{2+} levels is a downstream event of the interference with mitochondria, especially the production of ROS, by the removal of TC and the accumulation of Aβ aggregates in MC65 cells, and both events play some role in cell death. However, this does not rule out the possibility that the effects of Trolox on Ca^{2+} is through other mechanisms rather than ROS. Further detailed studies are warranted to understand the involvement of these two organelles in the death of MC65 cells.

Bivalent compound 17MN can readily pass into MC65 cells and colocalize with mitochondria and ER

Our results so far have suggested that 17MN may interact simultaneously with both mitochondria and ER to exert its neuroprotection in MC65 cells. To examine whether 17MN can localize at these organelles, a fluorescent analog of 17MN would be a helpful tool. Our previous SAR study demonstrated that modification of one of the phenolic oxygens of the curcumin moiety within the bivalent structure can maintain moderate neuroprotective

activity.[13] Therefore, we attached a nitro-benzoxadiazole (NBD) fluorescent tag onto one of the phenolic oxygens of the 17MN structure, yielding the designed probe 17MN-NBD (Figure 7A). After chemical synthesis of this probe, we first evaluated its neuroprotective activity in MC65 cells. As shown in Figure 7B, the EC_{50} of 17MN-NBD is 1.04 μM, a less than 5-fold decrease compared to the EC_{50} of 17MN (0.23 μM). The neuroprotective potency of 17MN is slightly less than the previously reported value, probably due to the employment of different batches of MC65 cells. More importantly, in the same cell populations, 17MN-NBD and 17MN showed equal protection at 3 μM. Given these results from the neuroprotective assay, we then examined the colocalization of 17MN-NBD in MC65 cells. To determine the subcellular destination of the probe, cells were co-stained with known mitochondrial- or ER-specific fluorescent dyes, Mitotracker Red and ERtracker Red, respectively. As shown in Figures 7C and 7D, 17MN-NBD is clearly able to penetrate the cell membrane and localize at both mitochondria and ER, thus suggesting that the bivalent compounds do indeed interact with these organelles to exhibit the observed effects on ΔΨm and Ca^{2+} mobilization.

DISCUSSION

Multiple pathogenic factors such as Aβ, calcium dyshomeostasis, mitochondria dysfunction, and inflammation have been suggested to contribute to the development of AD. Consequently, the multifactorial nature of AD makes drug discovery and development efforts for AD a challenging task. Recently, we have developed a bivalent strategy to incorporate the cell membrane/lipid rafts anchorage into our molecular design and a series of bivalent compounds have been developed. Biological characterization demonstrated that these bivalent compounds exhibited superior neuroprotection compared to either the single pharmacophore alone or the combination of both pharmacophores in a cellular model of AD.[13] In this study, we explored the possible mechanisms of action for these bivalent compounds using 17MN as a probe in MC65 cells.

Firstly, we demonstrated that MC65 cells die through a necroptotic mechanism under TC removal conditions, as reflected by the fact that a specific RIPK1 inhibitor, Nec-1, can dose dependently rescue MC65 cells from TC removal induced cytotoxicity. Although previous reports have demonstrated the association of the production of AβOs with the cell death of MC65 cells, studies with selective γ-secretase inhibitors would add more evidence to completely exclude the possibility of C99 expression on the cytotoxicity and necroptosis of MC65 cells upon TC removal. Our results also suggest that bivalent compound 17MN may protect MC65 cells by functioning between Aβ species and the RIPK1 as demonstrated by the results from MC65 and U937 cell studies.

Mitochondria and Ca^{2+} have been suggested to play some pathological roles in the development of AD, and crosstalk between mitochondria and ER, two main organelles that maintain the storage of Ca^{2+}, has also been proposed.[41, 45, 50] In this study, we established that ΔΨm and Ca^{2+} levels are increased upon the removal of TC in MC65 cells. As discussed above, in order to rule out the possible effects of C99 on ΔΨm and Ca^{2+} levels, further studies are warranted by employing a selective γ-secretase inhibitor under the same experimental conditions. Notably, our bivalent compound 17MN can reverse both of these

changes. Our studies also indicate that 17MN by itself does not induce significant change on $\Delta\Psi m$ and Ca^{2+} levels in MC65 cells in the presence of TC (data not shown), thus supporting the specific effects of 17MN on TC removal induced changes in MC65 cells. Further studies suggested that the interaction of AβOs with mitochondria can induce overproduction of ROS in a manner that is complex I independent. As a result of the oxidative stress from mitochondria, Ca^{2+} can be released from ER through an IP_3R dependent mechanism, thus leading to the rise of cytoplasmic Ca^{2+} levels. Since bivalent compound 17MN interferes with both events, we developed a fluorescent probe of 17MN to investigate the intracellular destination of 17MN. Confocal microscopy studies employing the fluorescent analog 17MN-NBD demonstrated that this probe can localize into both mitochondria and ER, consistent with the observed effects of 17MN on $\Delta\Psi m$ and Ca^{2+} levels.

In summary, our current studies along with previously reported results supported the notion that 17MN may exert its neuroprotective activity by interactions at multiple sites within MC65 cells, including moderate inhibitory effects on Aβ oligomerization, and interference with the interaction of AβOs with both mitochondria and ER.[13] These results suggest a multiple-site mechanism for 17MN in MC65 cells, consistent with our original design rationale and adding further evidence to support the development of effective disease-modifying agents for AD by small molecules with therapeutic polypharmacology.

Supplementary Material

Refer to Web version on PubMed Central for supplementary material.

Acknowledgments

We thank Dr. George M. Martin at the University of Washington, Seattle for kindly providing the MC65 cells. Microscopy was performed at the VCU - Dept. of Anatomy & Neurobiology Microscopy Facility, supported, in part, by funding from NIH-NINDS Center Core Grant 5 P30 NS047463 and, in part, by funding form NIH-NCI Cancer Center Support Grant P30 CA01605. The work was supported in part by the NIA of the NIH under award number R01AG041161 (S.Z.), CCTR Endowment Fund from VCU (Q.C.), and Department of Veterans Affairs Medical Research-Merit Review 1IO1BX001355-01A1 (E.L.).

References

1. Alzheimer’s Association. 2013 Alzheimer’s disease facts and figures. Alzheimers Dement. 2013; 9:208–245. [PubMed: 23507120]
2. Hardy J, Selkoe DJ. The amyloid hypothesis of Alzheimer’s disease: progress and problems on the road to therapeutics. Science. 2002; 297:353–356. [PubMed: 12130773]
3. Kirkitadze MD, Bitan G, Teplow DB. Paradigm shifts in Alzheimer’s disease and other neurodegenerative disorders: the emerging role of oligomeric assemblies. J Neurosci Res. 2002; 69:567–577. [PubMed: 12210822]
4. Walsh DM, Selkoe DJ. A beta oligomers - a decade of discovery. J Neurochem. 2007; 101:1172–1184. [PubMed: 17286590]
5. Selkoe DJ. Soluble oligomers of the amyloid beta-protein impair synaptic plasticity and behavior. Behav Brain Res. 2008; 192:106–113. [PubMed: 18359102]
6. Bush AI. Drug development based on the metals hypothesis of Alzheimer’s disease. J Alzheimers Dis. 2008; 15:223–240. [PubMed: 18953111]
7. Zhu X, Su B, Wang X, Smith MA, Perry G. Causes of oxidative stress in Alzheimer disease. Cell Mol Life Sci. 2007; 64:2202–2210. [PubMed: 17605000]

8. Eckert GP, Renner K, Eckert SH, Eckmann J, Hagl S, Abdel-Kader RM, Kurz C, Leuner K, Muller WE. Mitochondrial dysfunction--a pharmacological target in Alzheimer's disease. Mol Neurobiol. 2012; 46:136–150. [PubMed: 22552779]
9. Viegas-Junior C, Danuello A, da Silva Bolzani V, Barreiro EJ, Fraga CA. Molecular hybridization: a useful tool in the design of new drug prototypes. Curr Med Chem. 2007; 14:1829–1852. [PubMed: 17627520]
10. Tietze LF, Bell HP, Chandrasekhar S. Natural product hybrids as new leads for drug discovery. Angew Chem, Int Ed. 2003; 42:3996–4028.
11. Carreiras MC, Mendes E, Perry MJ, Francisco AP, Marco-Contelles J. The multifactorial nature of Alzheimer's disease for developing potential therapeutics. Curr Top Med Chem. 2013; 13:1745–1770. [PubMed: 23931435]
12. Lenhart JA, Ling X, Gandhi R, Guo TL, Gerk PM, Brunzell DH, Zhang S. "Clicked" bivalent ligands containing curcumin and cholesterol as multifunctional abeta oligomerization inhibitors: design, synthesis, and biological characterization. J Med Chem. 2010; 53:6198–6209. [PubMed: 20666513]
13. Liu K, Gandhi R, Chen J, Zhang S. Bivalent ligands targeting multiple pathological factors involved in Alzheimer's disease. ACS Med Chem Lett. 2012; 3:942–946. [PubMed: 23293731]
14. Sopher BL, Fukuchi K, Kavanagh TJ, Furlong CE, Martin GM. Neurodegenerative mechanisms in Alzheimer disease. A role for oxidative damage in amyloid beta protein precursor-mediated cell death. Mol Chem Neuropathol. 1996; 29:153–168. [PubMed: 8971693]
15. Sebastia J, Pertusa M, Vilchez D, Planas AM, Verbeek R, Rodriguez-Farre E, Cristofol R, Sanfeliu C. Carboxyl-terminal fragment of amyloid precursor protein and hydrogen peroxide induce neuronal cell death through different pathways. J Neural Transm. 2006; 113:1837–1845. [PubMed: 16752047]
16. Woltjer RL, McMahan W, Milatovic D, Kjerulf JD, Shie FS, Rung LG, Montine KS, Montine TJ. Effects of chemical chaperones on oxidative stress and detergent-insoluble species formation following conditional expression of amyloid precursor protein carboxy-terminal fragment. Neurobiol Dis. 2007; 25:427–437. [PubMed: 17141508]
17. Chinta SJ, Rane A, Yadava N, Andersen JK, Nicholls DG, Polster BM. Reactive oxygen species regulation by AIF- and complex I-depleted brain mitochondria. Free Radic Biol Med. 2009; 46:939–947. [PubMed: 19280713]
18. Meng P, Yoshida H, Tanji K, Matsumiya T, Xing F, Hayakari R, Wang L, Tsuruga K, Tanaka H, Mimura J, Kosaka K, Itoh K, Takahashi I, Kawaguchi S, Imaizumi T. Carnosic acid attenuates apoptosis induced by amyloid-beta 1-42 or 1-43 in SH-SY5Y human neuroblastoma cells. Neurosci Res. 2014 Epub ahead of print. 10.1016/j.neures.2014.12.003
19. Dong Y, Yang N, Liu Y, Li Q, Zuo P. The neuroprotective effects of phytoestrogen alpha-zearalanol on beta-amyloid-induced toxicity in differentiated PC-12 cells. Eur J Pharmacol. 2011; 670:392–398. [PubMed: 21946104]
20. Kim IK, Lee KJ, Rhee S, Seo SB, Pak JH. Protective effects of peroxiredoxin 6 overexpression on amyloid beta-induced apoptosis in PC12 cells. Free Radic Res. 2013; 47:836–846. [PubMed: 23937564]
21. Loo DT, Copani A, Pike CJ, Whittemore ER, Walencewicz AJ, Cotman CW. Apoptosis is induced by beta-amyloid in cultured central nervous system neurons. Proc Natl Acad Sci USA. 1993; 90:7951–7955. [PubMed: 8367446]
22. Troy CM, Rabacchi SA, Xu Z, Maroney AC, Connors TJ, Shelanski ML, Greene LA. beta-Amyloid-induced neuronal apoptosis requires c-Jun N-terminal kinase activation. J Neurochem. 2001; 77:157–164. [PubMed: 11279271]
23. Kienlen-Campard P, Miolet S, Tasiaux B, Octave JN. Intracellular amyloid-beta 1-42, but not extracellular soluble amyloid-beta peptides, induces neuronal apoptosis. J Biol Chem. 2002; 277:15666–15670. [PubMed: 11861655]
24. Chojnacki JE, Liu K, Yan X, Toldo S, Selden T, Estrada M, Rodriguez-Franco MI, Halquist MS, Ye D, Zhang S. Discovery of 5-(4-hydroxyphenyl)-3-oxo-pentanoic acid [2-(5-methoxy-1H-indol-3-yl)-ethyl]-amide as a neuroprotectant for Alzheimer's disease by hybridization of curcumin and melatonin. ACS Chem Neurosci. 2014; 5:690–699. [PubMed: 24825313]

25. Kamata H, Honda S, Maeda S, Chang L, Hirata H, Karin M. Reactive oxygen species promote TNFalpha-induced death and sustained JNK activation by inhibiting MAP kinase phosphatases. Cell. 2005; 120:649–661. [PubMed: 15766528]
26. Vandenabeele P, Galluzzi L, Vanden Berghe T, Kroemer G. Molecular mechanisms of necroptosis: an ordered cellular explosion. Nat Rev Mol Cell Biol. 2010; 11:700–714. [PubMed: 20823910]
27. Marshall KD, Baines CP. Necroptosis: is there a role for mitochondria? Front Physiol. 2014; 5:323. [PubMed: 25206339]
28. Degterev A, Huang Z, Boyce M, Li Y, Jagtap P, Mizushima N, Cuny GD, Mitchison TJ, Moskowitz MA, Yuan J. Chemical inhibitor of nonapoptotic cell death with therapeutic potential for ischemic brain injury. Nat Chem Biol. 2005; 1:112–119. [PubMed: 16408008]
29. Li M, Beg AA. Induction of necrotic-like cell death by tumor necrosis factor alpha and caspase inhibitors: novel mechanism for killing virus-infected cells. J Virol. 2000; 74:7470–7477. [PubMed: 10906200]
30. Maezawa I, Hong HS, Wu HC, Battina SK, Rana S, Iwamoto T, Radke GA, Pettersson E, Martin GM, Hua DH, Jin LW. A novel tricyclic pyrone compound ameliorates cell death associated with intracellular amyloid-beta oligomeric complexes. J Neurochem. 2006; 98:57–67. [PubMed: 16805796]
31. Tillement L, Lecanu L, Papadopoulos V. Alzheimer's disease: effects of beta-amyloid on mitochondria. Mitochondrion. 2011; 11:13–21. [PubMed: 20817045]
32. Devi L, Prabhu BM, Galati DF, Avadhani NG, Anandatheerthavarada HK. Accumulation of amyloid precursor protein in the mitochondrial import channels of human Alzheimer's disease brain is associated with mitochondrial dysfunction. J Neurosci. 2006; 26:9057–9068. [PubMed: 16943564]
33. Fukui M, Choi HJ, Zhu BT. Rapid generation of mitochondrial superoxide induces mitochondrion-dependent but caspase-independent cell death in hippocampal neuronal cells that morphologically resembles necroptosis. Toxicol Appl Pharmacol. 2012; 262:156–166. [PubMed: 22575170]
34. Ye YC, Wang HJ, Yu L, Tashiro S, Onodera S, Ikejima T. RIP1-mediated mitochondrial dysfunction and ROS production contributed to tumor necrosis factor alpha-induced L929 cell necroptosis and autophagy. Int Immunopharmacol. 2012; 14:674–682. [PubMed: 23000518]
35. Qiao H, Koya RC, Nakagawa K, Tanaka H, Fujita H, Takimoto M, Kuzumaki N. Inhibition of Alzheimer's amyloid-beta peptide-induced reduction of mitochondrial membrane potential and neurotoxicity by gelsolin. Neurobiol Aging. 2005; 26:849–855. [PubMed: 15718043]
36. Koopman WJ, Nijtmans LG, Dieteren CE, Roestenberg P, Valsecchi F, Smeitink JA, Willems PH. Mammalian mitochondrial complex I: biogenesis, regulation, and reactive oxygen species generation. Antioxid Redox Signal. 2010; 12:1431–1470. [PubMed: 19803744]
37. Zorov DB, Juhaszova M, Yaniv Y, Nuss HB, Wang S, Sollott SJ. Regulation and pharmacology of the mitochondrial permeability transition pore. Cardiovasc Res. 2009; 83:213–225. [PubMed: 19447775]
38. Rao VK, Carlson EA, Yan SS. Mitochondrial permeability transition pore is a potential drug target for neurodegeneration. Biochim Biophys Acta. 2014; 1842:1267–1272. [PubMed: 24055979]
39. Martin LJ. Olesoxime, a cholesterol-like neuroprotectant for the potential treatment of amyotrophic lateral sclerosis. IDrugs. 2010; 13:568–580. [PubMed: 20721828]
40. Zorov DB, Juhaszova M, Sollott SJ. Mitochondrial reactive oxygen species (ROS) and ROS-induced ROS release. Physiol Rev. 2014; 94:909–950. [PubMed: 24987008]
41. Lemasters JJ, Qian T, Elmore SP, Trost LC, Nishimura Y, Herman B, Bradham CA, Brenner DA, Nieminen AL. Confocal microscopy of the mitochondrial permeability transition in necrotic cell killing, apoptosis and autophagy. Biofactors. 1998; 8:283–285. [PubMed: 9914830]
42. Bernardi P, Vassanelli S, Veronese P, Colonna R, Szabo I, Zoratti M. Modulation of the mitochondrial permeability transition pore. Effect of protons and divalent cations. J Biol Chem. 1992; 267:2934–2939. [PubMed: 1737749]
43. Demuro A, Parker I, Stutzmann GE. Calcium signaling and amyloid toxicity in Alzheimer disease. J Biol Chem. 2010; 285:12463–12468. [PubMed: 20212036]

44. Resende R, Ferreiro E, Pereira C, Resende de Oliveira C. Neurotoxic effect of oligomeric and fibrillar species of amyloid-beta peptide 1-42: involvement of endoplasmic reticulum calcium release in oligomer-induced cell death. Neuroscience. 2008; 155:725–737. [PubMed: 18621106]

45. Ma HT, Venkatachalam K, Parys JB, Gill DL. Modification of store-operated channel coupling and inositol trisphosphate receptor function by 2-aminoethoxydiphenyl borate in DT40 lymphocytes. J Biol Chem. 2002; 277:6915–6922. [PubMed: 11741932]

46. Ma HT, Patterson RL, van Rossum DB, Birnbaumer L, Mikoshiba K, Gill DL. Requirement of the inositol trisphosphate receptor for activation of store-operated Ca2+ channels. Science. 2000; 287:1647–1651. [PubMed: 10698739]

47. Paillard M, Tubbs E, Thiebaut PA, Gomez L, Fauconnier J, Da Silva CC, Teixeira G, Mewton N, Belaidi E, Durand A, Abrial M, Lacampagne A, Rieusset J, Ovize M. Depressing mitochondria-reticulum interactions protects cardiomyocytes from lethal hypoxia-reoxygenation injury. Circulation. 2013; 128:1555–1565. [PubMed: 23983249]

48. Garcia-Perez C, Schneider TG, Hajnoczky G, Csordas G. Alignment of sarcoplasmic reticulum-mitochondrial junctions with mitochondrial contact points. Am J Physiol Heart Circ Physiol. 2011; 301:H1907–1915. [PubMed: 21856920]

49. Szabadkai G, Bianchi K, Varnai P, De Stefani D, Wieckowski MR, Cavagna D, Nagy AI, Balla T, Rizzuto R. Chaperone-mediated coupling of endoplasmic reticulum and mitochondrial Ca^{2+} channels. J Cell Biol. 2006; 175:901–911. [PubMed: 17178908]

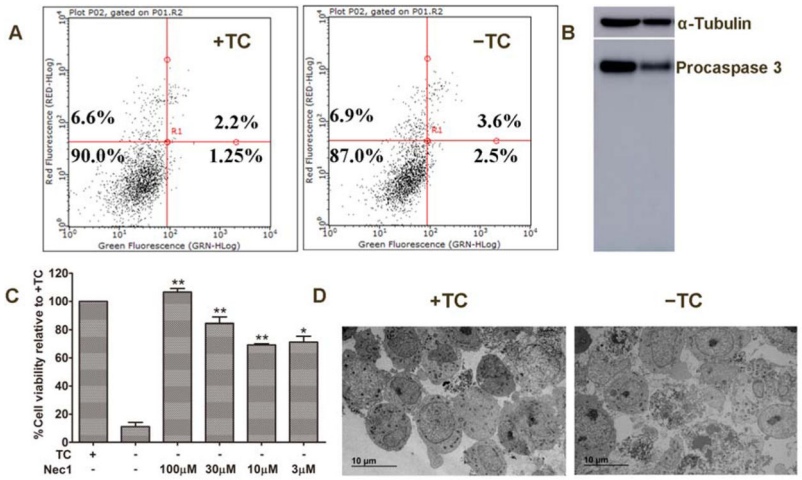

Figure 1.

MC65 cells die through necroptosis after TC removal. A) MC65 cells under +TC or −TC conditions for 48 h were stained with PI and Annexin V-FITC, and analyzed by flow cytometry. B) MC65 cells were incubated under +TC or −TC conditions for 48 h. Lysates from cultures were analyzed by Western blotting using a caspase 3 antibody. C) MC65 cells were treated with Necrostatin-1 at indicated concentrations under −TC condition for 72 h. Cell viability was assessed by MTT assay. (*$p < 0.05$, **$p < 0.01$ compared to −TC). D) TEM images of necrotic cell death induced under −TC conditions.

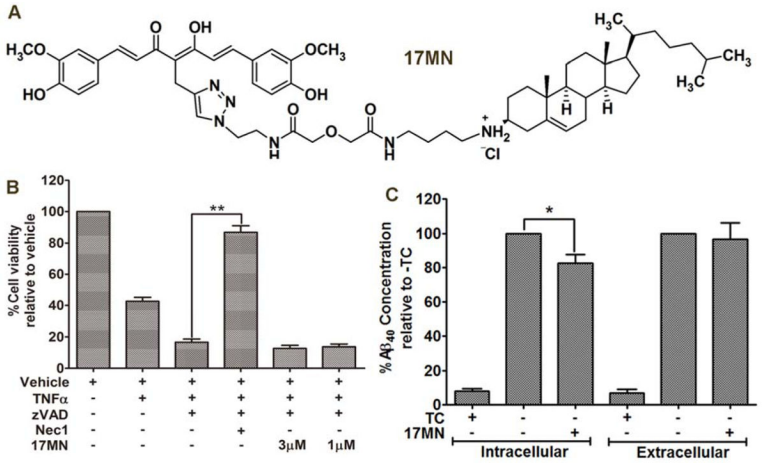

Figure 2.

17MN functions upstream of RIPK1 in MC65 cells. A) Chemical structure of 17MN. B) U937 cells were pretreated with 17MN (1 or 3 μM) or Necrostatin-1 (10 μM) and pan caspase inhibitor zVAD (10 μM) for 1 h, then TNF-α (50 ng/mL) was added and incubated for 72 h. Cell viability was assessed by MTT assay. (**$p < 0.01$). C) MC65 cells were treated with 17MN (1 μM) under −TC conditions for 48 h. Medium was collected for analysis of extracellular $A\beta_{40}$. Cells were lysed and analyzed for intracellular $A\beta_{40}$. Total $A\beta_{40}$ concentrations were normalized by total protein content of lysed cells. (*$p < 0.05$).

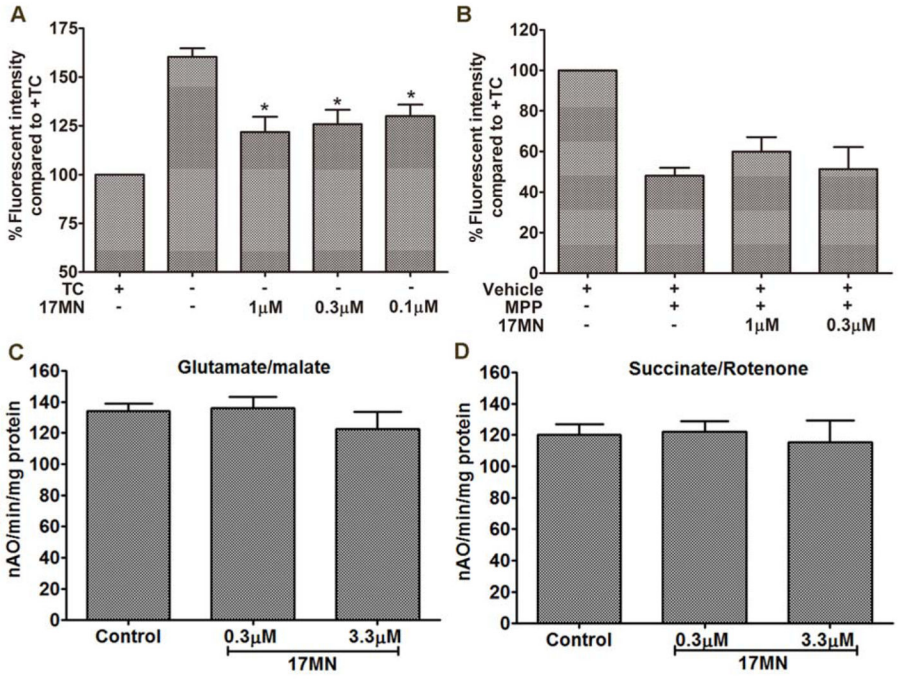

Figure 3.

The influence of 17MN on mitochondrial membrane potential. A) MC65 cells were treated with 17MN at indicated concentrations under −TC condition for 48 h. Cells were then incubated with TMRM (100 nM) for 30 min. Mean fluorescence intensity was measured by flow cytometry. (*$p < 0.05$ compared to −TC). B) SH-SY5Y cells were treated with 17MN (1 and 0.3 μM) and MPP^+ (2.5 mM) for 24 h. Cells were then incubated with TMRM (100 nM) for 30 min. Mean fluorescence intensity was measured by flow cytometry. C and D) Oxygen consumption in mitochondria was measured using a Clark-type oxygen electrode at 30 °C using glutamate/malate (C) and using succinate/rotenone (D) in the presence or absence of 17MN.

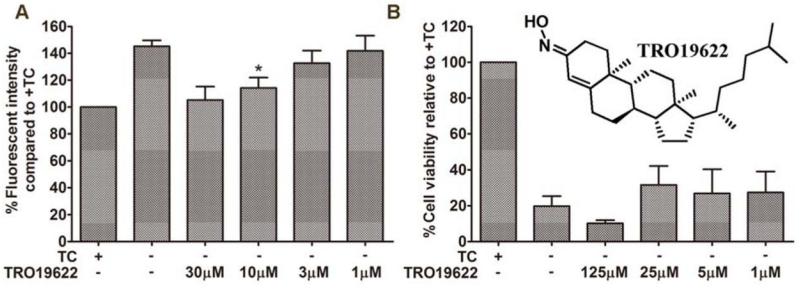

Figure 4.

TRO19622 suppressed −TC induced ΔΨm increase, but didn't show protection in MC65 cells. A) MC65 cells were treated with TRO19622 at indicated concentrations under −TC conditions for 48 h. Cells were then incubated with TMRM (100 nM) for 30 min. Mean fluorescence intensity was measured by flow cytometry. (*$p < 0.05$). B) MC65 cells were treated with TRO19622 at indicated concentrations under −TC condition for 72 h. Cell viability was assessed by MTT assay.

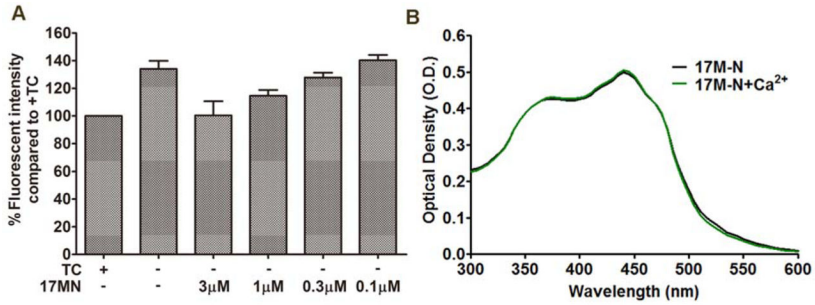

Figure 5.

17MN suppressed the cytosolic Ca^{2+} rise in MC65 cells under −TC conditions. A) MC65 cells were treated with 17MN at indicated concentrations under −TC conditions for 48 h. Cells were then incubated with Fluo-4AM (2 μM) for 30 min. Mean fluorescence intensity was measured by flow cytometry. B) 17MN (50 μM) was incubated with $CaCl_2$ (60 μM) at room temperature for 10 min, then the UV-vis spectrum was recorded from 300 nm to 600 nm.

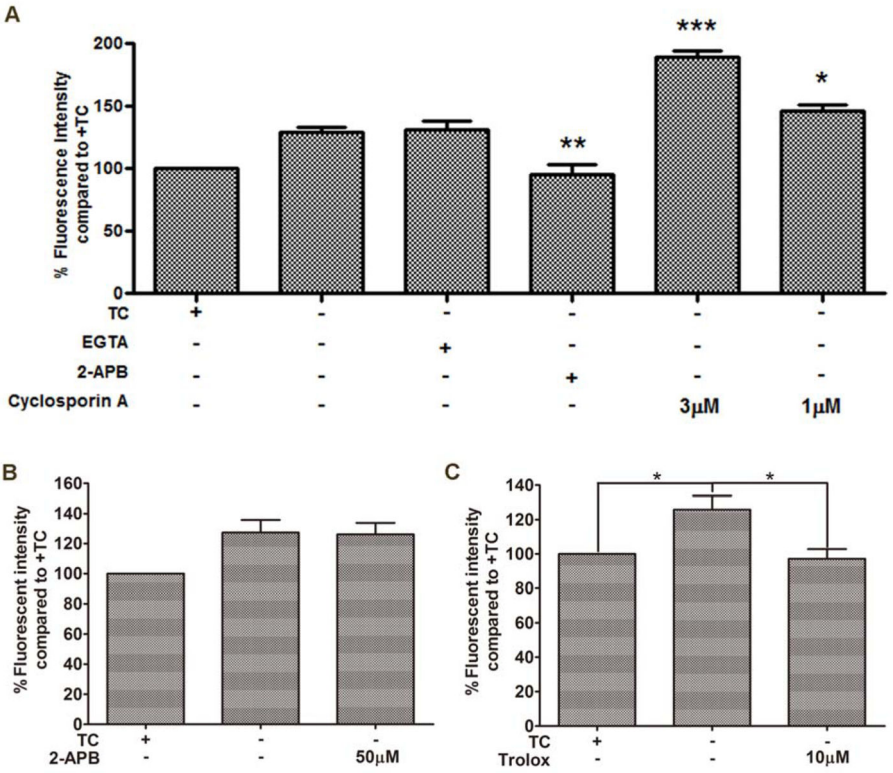

Figure 6.

Calcium mobilization from ER and MMP change of mitochondria are related in MC65 cells under −TC conditions. A) MC65 cells were treated with indicated compounds under −TC condition for 48 h. Cells were then incubated with Fluo-4AM (2 μM) for 30 min. Mean fluorescence intensity was measured by flow cytometry. (*$p < 0.05$, **$p < 0.01$, ***$p < 0.001$). B) MC65 cells were treated with 2-APB (50 μM) under −TC condition for 48 h. Cells were then incubated with TMRM (100 nM) for 30 min. Mean fluorescence intensity was measured by flow cytometry. C) MC65 cells were treated with Trolox (10 μM) under −TC condition for 48 h. Cells were then incubated with Fluo-4AM (2 μM) for 30 min. Mean fluorescence intensity was measured by flow cytometry (*$p < 0.05$).

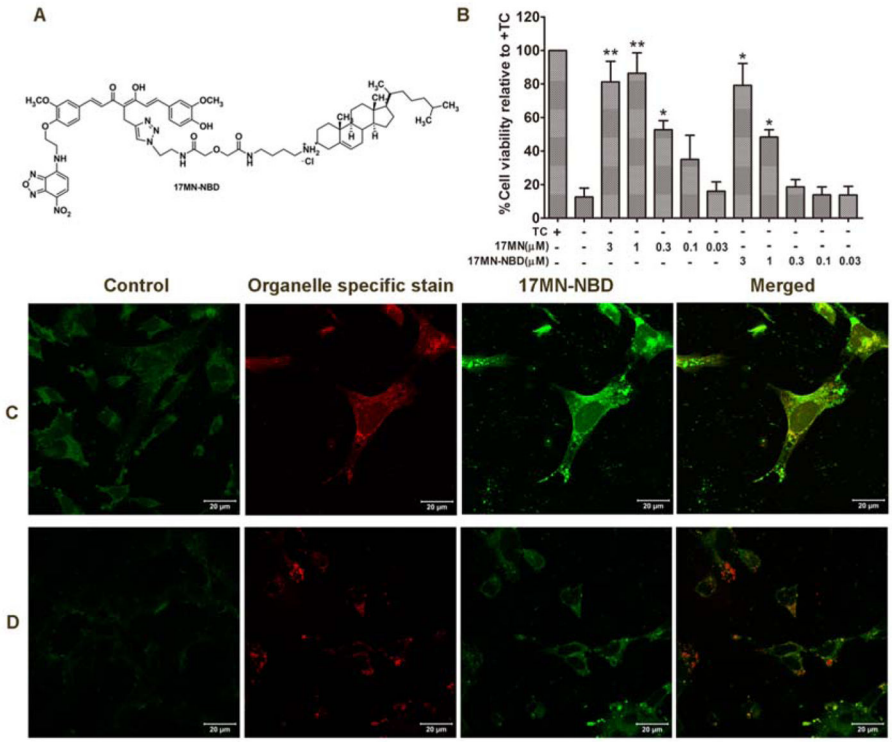

Figure 7.

17MN-NBD localized to the mitochondria and ER of MC65 cells. A) Chemical structure of 17MN-NBD. B) MC65 cells were treated with 17MN or 17MN-NBD at indicated concentrations under −TC condition for 72 h. Cell viability was assessed by MTT assay. C and D) MC65 cells grown on cover slides were treated with 17MN-NBD (3 μM) and Mitotracker Red (300 nM) (C) or ERtracker Red (1 μM) (D). Cells were fixed with 4% formaldehyde and visualized by LSM710 confocal microscopy.